Mechanical properties of porous metastable beta Ti-Nb-Zr alloys for biomedical applications

Braïlovski, V.; Prokoshkin, S.; Gauthier, M.; Inaekyan, K.; Dubinskiy, S.

Publisher's version / Version de l'éditeur:
https://doi.org/10.1016/j.jallcom.2011.12.157
Journal of alloys and compounds, 577, Supplement 1, pp. S413-S417, 2012-02-06

MECHANICAL PROPERTIES OF POROUS METASTABLE BETA Ti-Nb-Zr ALLOYS FOR BIOMEDICAL APPLICATIONS

V. Brailovski[(1)], S. Prokoshkin [(2)], M. Gauthier[(3)], K. Inaekyan[(1)], S. Dubinskiy [(1,2)]

(1) Ecole de Technologie Superieure, 1100, Notre-Dame Street West, Montreal (Quebec), H3C 1K3 Canada

(2) National University of Science and Technology "MISIS", Leninskiy prosp. 4, Moscow 119049, Russian Federation

(3) Industrial Materials Institute (IMI), National Research Council, Government of Canada, 75, de Mortagne, Boucherville (Quebec), J4B 6Y4 Canada

vbrailovski@etsmtl.ca, prokoshkin@tmo.misis.ru, maxime.gauthier@imi.cnrc-nrc.gc.ca, karine.inaekyan@etsmtl.ca, sergey.dubinskiy@ens.etsmtl.ca

Keywords: metals and alloys, powder metallurgy, sintering, mechanical properties, shape memory

Abstract. For this study, Ti-(20...22)Nb-(5...6)Zr (at%) ingots were manufactured by vacuum and argon arc melting. The obtained ingots were divided into two batches: the first subjected to cold rolling (CR) from 30 to 85% of thickness reduction, and subsequent annealing in the 450 to 600°C temperature range (1h). Regardless of the CR intensity, Ti-Nb-Zr samples subjected to 600°C annealing showed the highest fatigue resistance during room-temperature cumulative cycling due to the stress-induced martensitic transformation occurring in the polygonized dislocation substructure (average subgrain size ~ 100 nm). The second batch was atomized to produce 100-micron-size powders in order to manufacture open-cell porous material (cell size vary from 136 to 561 microns) of 46% porosity by means of powder metallurgy using a polymer-based foaming process. Tensile, compression and bending testing were performed at RT on foam samples annealed at 450 to 600°C (1h). Results indicated that Young's modulus of Ti-Nb-Zr foams significantly decreases as compared to the as-sintered material: when annealing temperature increases from 450 to 600°C, Young's modulus decreases from 10±2 GPa to 6±1 GPa. Under the same testing conditions, Ti-CP foams produced by the same technology and having similar porosity remain fairly insensible to post-sintering annealing.

1. Introduction

The need for a metallic implant material combining superelasticity with a biocompatibility comparable to that of pure titanium represents the main incentive for ongoing research in the field of β-type Ti-based superelastic alloys [1]-[6]. Ternary and quaternary Ti-Nb-based alloys have been extensively investigated over the last ten years and the results confirm the possibility of producing Ni-free, Ti-based alloys with superelasticity thanks to reversible β to α″ martensitic transformation [7]. Efforts to alloy binary Ti-Nb alloys with a third element, such as Ta or Zr were undertaken with the objectives of stabilizing the β phase at room temperature, creating conditions for α″ phase formation, decreasing the Young modulus, and promoting solid solution hardening, thereby improving the Ni-free titanium alloys' shape memory properties [8].

Thermal treatment of the ternary alloys consists of the simultaneous softening caused by the recovery, the polygonization of β-phase austenite structure after work hardening and the hardening caused by the ω-, α-precipitations [9]. As well as precipitation processes, the enrichment by interstitial atoms (oxygen, nitrogen, etc.) during annealing and quenching plays an important role in β↔α'' martensitic transformation responsible for shape memory effects.

In the same vein, in our work on thermomechanical processing of Ti-(20…22)Nb-(5…6)Zr (at%) shape memory alloys [10], significant softening due to β↔α'' stress-induced martensitic transformation was observed after post-deformation annealing at 600°C (1h), regardless of the cold-work intensity (Figure 1).

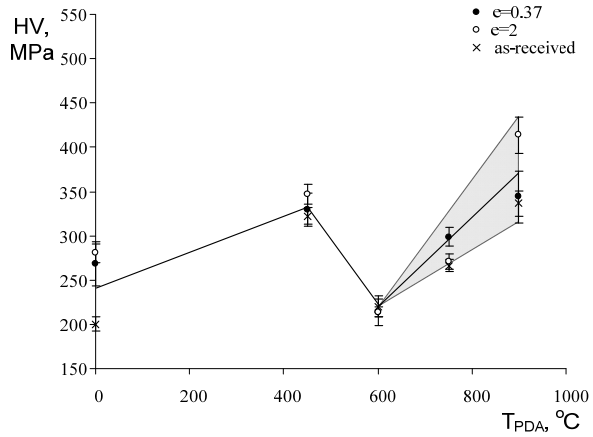

Figure 1. Microhardness of Ti-20.5Nb-5.6Zr alloy (at.%) alloy as a function of the cold rolling (CR) true strain thickness reduction and the temperature of post-deformation annealing (PDA) [10].

Furthermore, the thermomechanical processing of these alloys was optimized [11]: CR e=0.37 and PDA 600°C, 30 min, in terms of the closeness of the alloy's mechanical behavior to the conventional superelasticity and the number of cycles to failure (see Figure 2a). Note that the microstructure of this material corresponds to the β-phase polygonized nanosubgrained structure with average subgrain size somewhat below 100 nm (see [12] for a detailed microstructural analysis). The alloy subjected to these optimum processing conditions was then subjected to isothermal ten-cycle 2% strain cumulative tensile testing followed by monotonous tension up to specimen failure in the -140…150°C temperature range (Figure 2b).

From the results of the isothermal tensile testing, it was concluded that for this alloy, perfectly superelastic behavior with the lowest transformation yield stress and Young's modulus and the highest elongation to failure, corresponds to a testing temperature of T = –75°C. It also became clear that the upper bound of the superelastic window for this material is situated around RT [11].

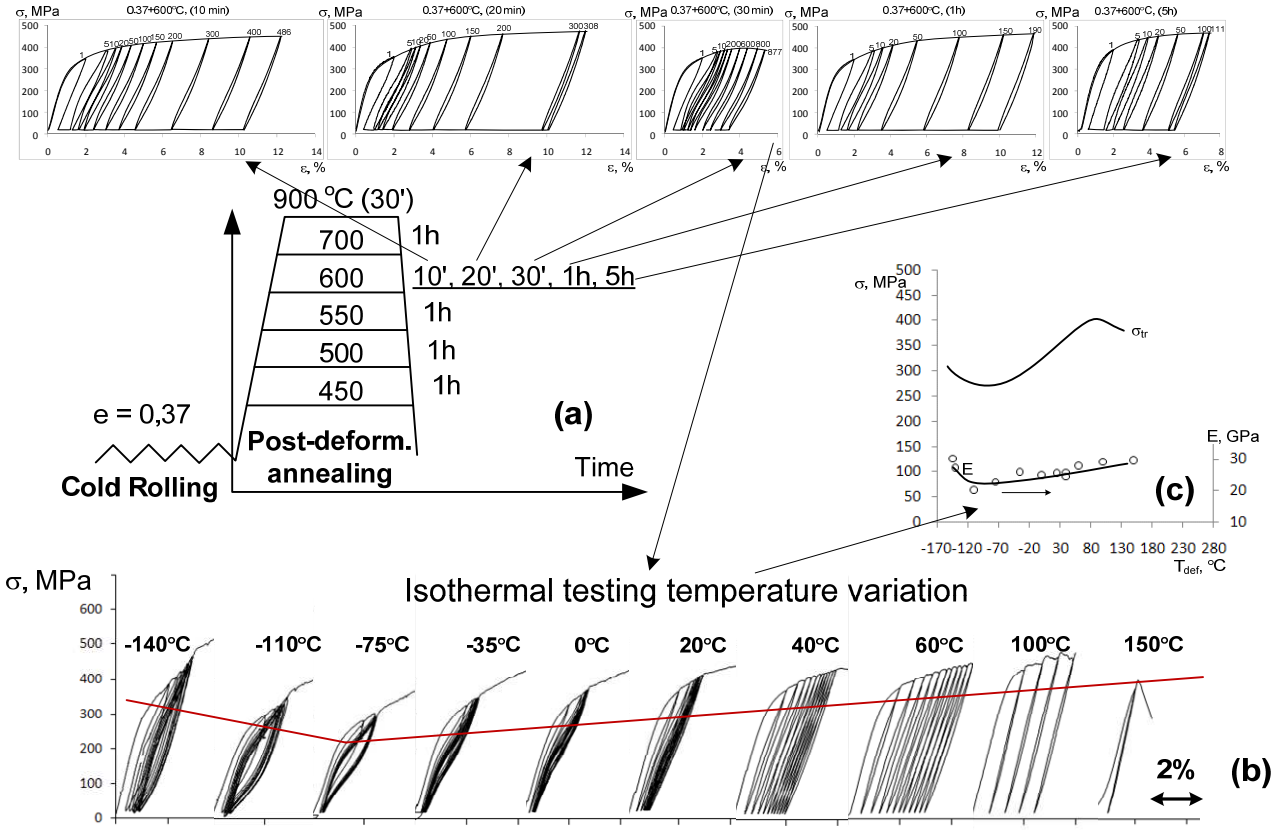

Figure 2. a) Mechanical behavior of Ti-22Nb-6Zr alloy as a function of PDA time (a) and testing temperature (b,c), adapted from [10]-[11]

Since the bulk material of this composition subjected to 600°C (1h) annealing showed significant softening at RT regardless of the cold work intensity (e=0 to 2), attributed to β↔α'' martensitic transformation, it is reasonable to suggest that the foams produced from this alloy would be equally sensitive to thermal treatment as their parent material. The main objective of the current work is to verify the last hypothesis and confirm the possibility of regulating the mechanical behavior of metastable beta titanium alloy foams using post-sintering heat treatment.

2. Materials and methods

2.1 Foam manufacturing

Ti-20.8Nb-5.5Zr and Ti-20.5Nb-5.6Zr (at.) ingots (50 mm diameter, 660 mm long) were manufactured by Vacuum Arc Remelting (VAR) by the Flowserve Corp. (USA) [11]. The obtained ingots were atomized by TLS Technik Spezialpulver (Germany). Cylindrical foam samples (∅13×30mm) with target porosity of ≈46% were manufactured using an original powder metallurgy process by IMI-CNRC (see image and chart of the pore distribution for a 46% porosity sample in Figure 3 and the numbers in Table 1) [13]. Figure 4 shows the impurity content variations from bulk to foam product.

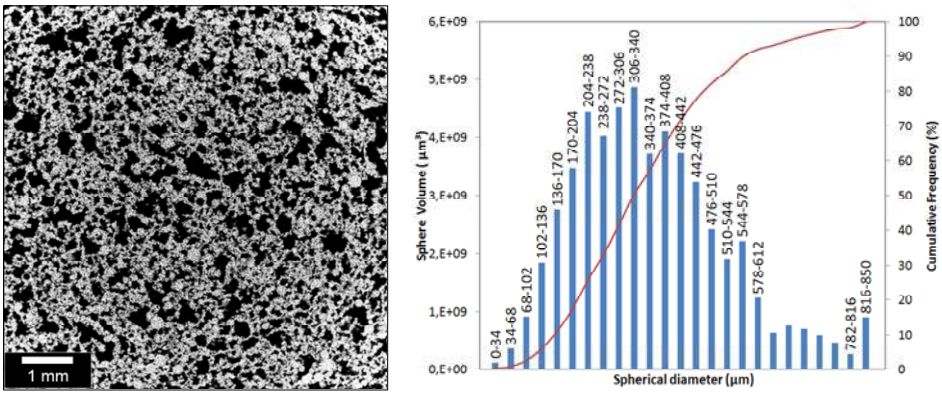

Figure 3 Tomographic analysis of Ti-20.9Nb-5.5Zr foams with 45.66 (0.18)% porosity [10]

Table 1. Foams characteristics [10]

Foam Porosity* (%)	**Open (Closed) Porosity** (%)**	**Average Foam Porosity[§] (with standard deviation) (%)**	**Pore size distribution parameters[§]**		
			d_{10} (µm)	**d_{50} (µm)**	**d_{90} (µm)**
45.84	45.66 (0.18)	45.11 ± 1.02	136	306	561
* Calculated from sample dimensions and mass; ** He-gas pycnometry; [§] Tomography / Image analysis					

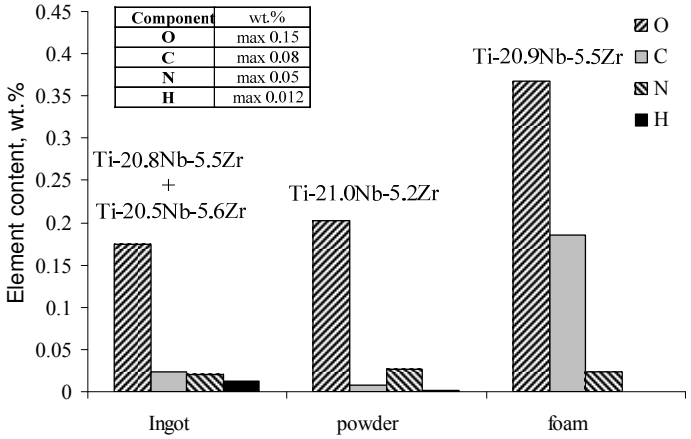

Figure 4 Impurity content in Ti-Nb-Zr ingots, powder and foams

The foam specimens were encapsulated in Ar-filled quartz tubes and annealed in an open air furnace (PYRADIA) at 450°C and 600°C (1h) with subsequent water quenching. For the sake of comparison, Ti-CP (commercial purity) foams (46% porosity) were produced following the same technological route ingots→powder→foam as Ti-Nb-Zr, and were encapsulated inside the same quartz tubes for thermal treatment and quenching.

2.2 Foam characterization

X-ray analysis was performed at RT using a PANALYTICAL X'Pert Pro diffractometer ($\lambda_{CuK\alpha}$ =1.541874 Å).

Mechanical testing was performed at RT under three testing modes: a) tensile testing, b) three-point bending and c) compression testing. An MTS Minibionix 858 was used for compression testing (at a $0.002s^{-1}$ strain rate) and an EnduraTEC ELF 3200 was used for tensile (at a $0.002s^{-1}$ strain rate) and three-point bending testing (0.0005 s^{-1} strain rate).

Specimens for mechanical testing were cut from the massive foam samples using a low-speed diamond saw. Tensile and three-point bending tests were performed on prismatic specimens with a cross section area of about 1×1 (mm) and 3×3 (mm) and 20 mm long. Compression testing was performed on prismatic specimens with the following dimensions: 3×3×3 (width, thickness, height, mm).

Monotonous cycling (maximum 10 cycles) was carried out for up to 1.2% in bending strain, up to 0.5% in tensile strain and up to 4, 8 and 20% in compression strain, and at each strain level was cycled 10 times. Apparent engineering uniaxial stress and strain in the tension and compression of the foam specimens were calculated using standard formulas. The apparent stress and strain on the outer fiber of the foam specimens during three-point bending were calculated as follows:

$$\sigma = \frac{3Fl}{2bh^2}; \varepsilon = \frac{6h\delta}{l^2},$$

where F is the force at a given point of the load-deflection curve, l is the span between supports, b and h are the specimen's width and thickness and δ is the maximum specimen deflection.

3. Results

Figure 5 contains X-ray diffractograms of Ti-CP and Ti-Nb-Zr foams in as-received and annealed states. At RT, Ti-CP foam has an α-phase structure (Figure 5 b), whereas Ti-Nb-Zr foam has a β-phase austenite structure (Figure 5 a). No notable differences between the diffractograms of the as-sintered and annealed samples can be distinguished. Consequently, during mechanical testing of as-sintered and annealed foams, it is expected that conventional elasto-plastic behavior of Ti-CP samples and partially superelastic behavior of Ti-Nb-Zr samples would be possible to observe, the latter due to reversible β-austenite to α''-martensite transformation.

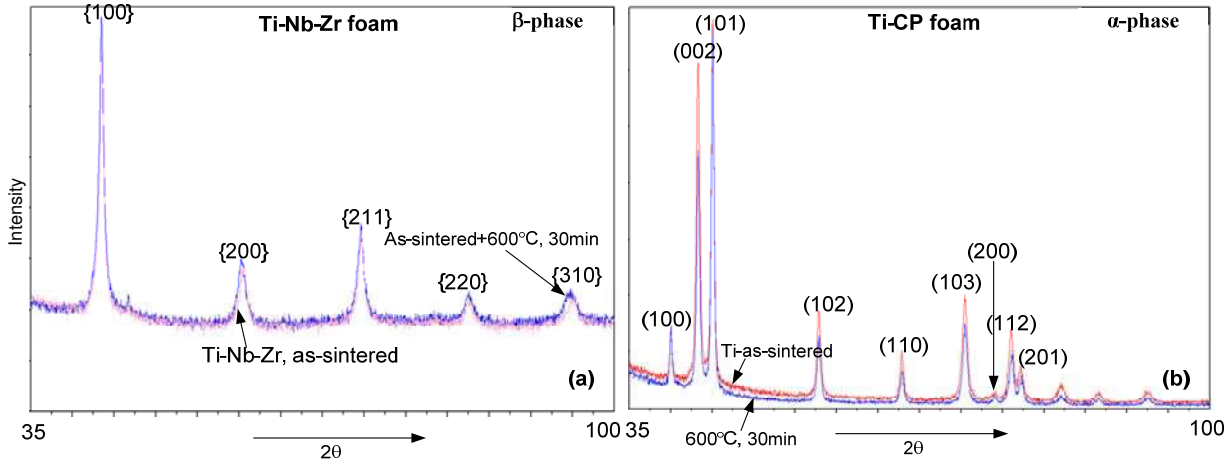

Figure 5. X-ray diffractograms of as-sintered and 600°C (30 min) annealed Ti-Nb-Zr and Ti-CP foams

The stress-strain diagrams of Ti-Nb-Zr foams obtained during tensile, three-point bending and compression testing are presented in Figure 6 and Figure 7. Note that the maximum strain reached during each testing mode was limited to avoid specimen failure.

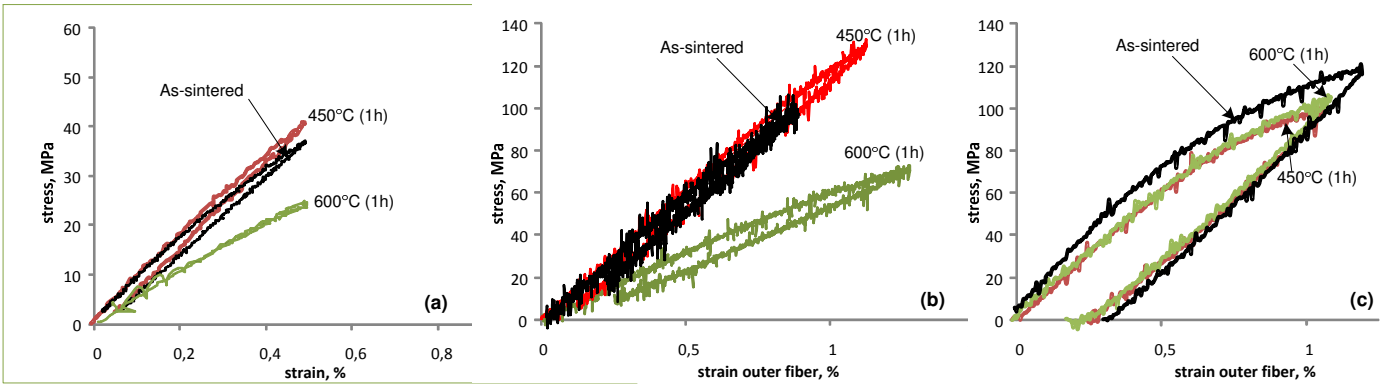

Figure 6. Tensile (a) and three-point bending testing of Ti-Nb-Zr (b) and Ti-CP (c) foams

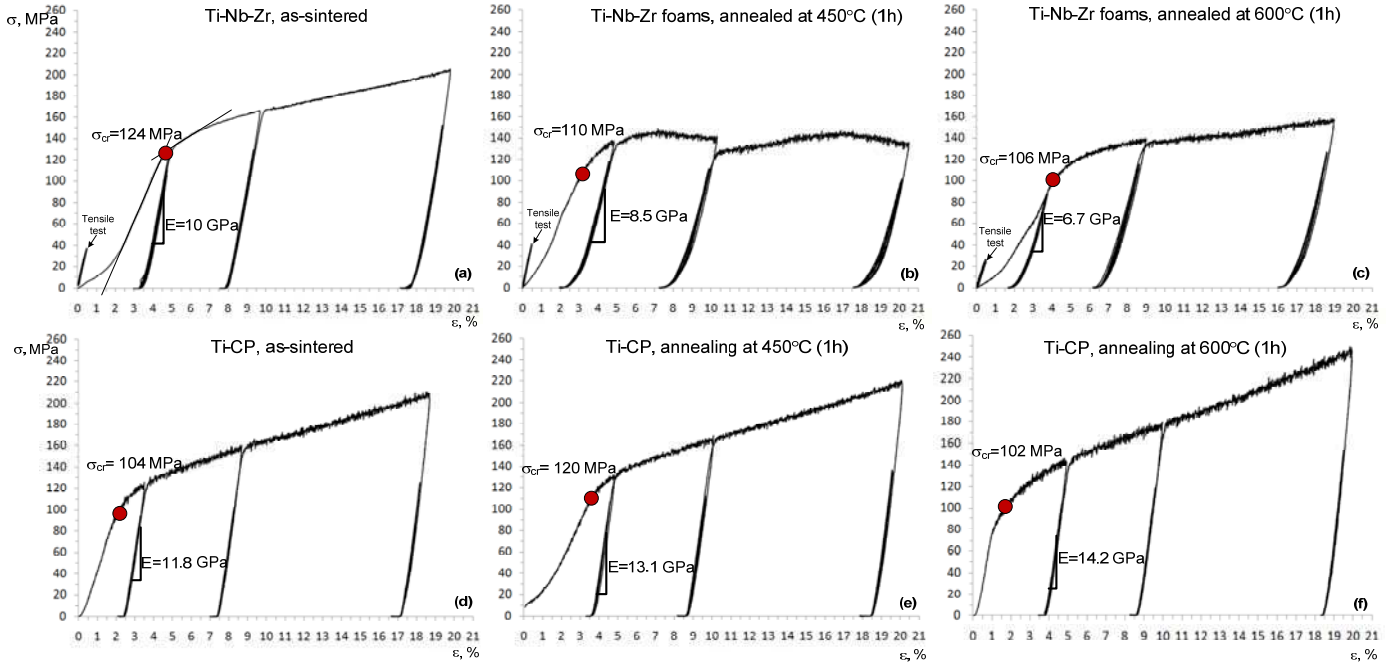

Figure 7. Compression testing of Ti-Nb-Zr (a-c) and Ti-CP (d-f) foams: (a, d) as-sintered; (b, e) annealed at 450°C (1h); (c, f) annealed at 600°C (1h).

4. Discussion

It is observed that Ti-Nb-Zr and Ti-CP foams demonstrate different sensitivity to post-sintering thermal treatment, and that this is an observable difference, despite the similarity of their X-ray diffractograms before and after annealing. The higher the annealing temperature, the less the apparent stiffness of Ti-Nb-Zr foams (Figure 6a, b and Figure 7 a-c), whereas Ti-CP behavior is almost not affected at all (Figure 6 c and Figure 7 d-f).

The influence of post-sintering thermal treatment on the tensile and three-point bending stress-strain diagrams of Ti-Nb-Zr and Ti-CP foams is quite different (Figure 6, Figure 7). Moreover, under tensile and three-point bending testing modes, Ti-Nb-Zr foams manifest linear superelastic behavior (Figure 6 a,b), whereas Ti-CP foams' behavior is elasto-plastic (large hysteresis, significant residual strains), as shown in Figure 6 c.

Compression testing of Ti-Nb-Zr foams also shows the significant influence of the post-sintering thermal treatment on the onset stress and apparent Young's modulus, which is evidently not the case with Ti-CP foams (Figure 7). Note that the macroscopic behavior of foam structures depends on the intrinsic behavior of the foam material and its spatial organization (foam architecture), and is therefore much more complicated than in the case of bulk material. An apparent non-linearity on the unloading compression stress-strain diagrams of Ti-Nb-Zr foams can be observed, which is believed to be a sign of the local superelastic behavior.

Figure 8 illustrates the evolution of the Ti-Nb-Zr foams' apparent Young's modulus measured on the unloading portions of the stress-strain diagrams for all of the testing modes as a function of annealing temperature. Note that the first loading part of the compression stress-strain diagram cannot be considered as a "true" mechanical behavior because of the possible localized plasticity in the specimen at stresses well below the compressive strength of the foam, which could reduce the slope of the loading curve [14].

Generally speaking, for Ti-Nb-Zr foams, the higher the annealing temperature, the lower the Young's modulus: the highest Young's modulus is observed with the as-sintered material (8-12 GPa) and the lowest after annealing at 600°C (5-7 GPa). As for Ti-CP foams, their apparent Young's modulus remains stable regardless of the heat treatment conditions: it varies between 10 and 14 GPa depending on the deformation mode.

It should also be noted that heat treatment of the Ti-CP and Ti-Nb-Zr foams could bring different factors into play: the phase state of the material, the size of structural elements, the quantity of interstitial elements due to limited purity of annealing atmosphere, etc. These factors could act differently in respect to the material's mechanical characteristics. Moreover, the pore's size and distribution, sample size and preparation could also explain the apparent influence of the deformation mode on the Young's modulus presented in Figure 8.

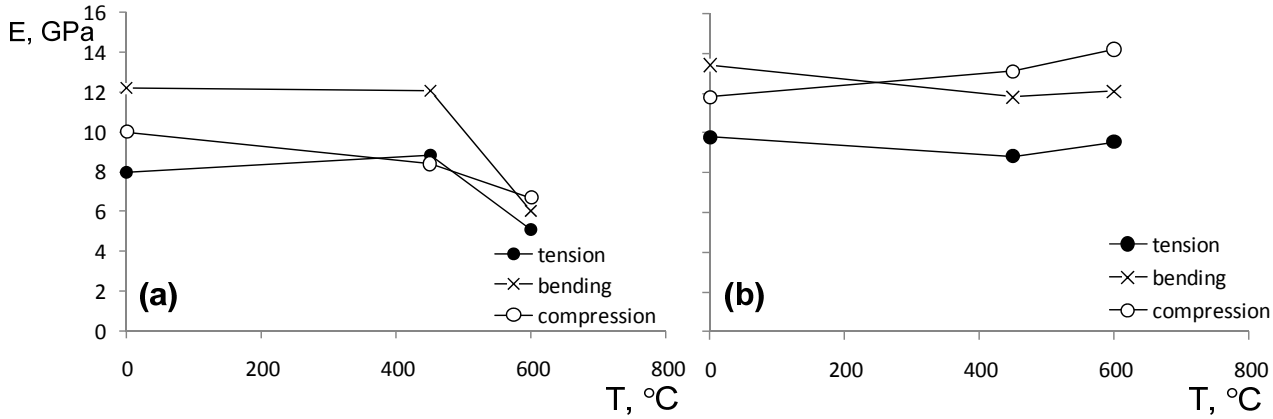

Figure 8. Young's modulus of Ti-Nb-Zr (a) and Ti-CP (b) foams measured upon unloading under tension, bending and compression deformation modes

5. Conclusions

The elasto-plastic mechanical behavior of Ti-CP foams with given characteristics of pore size and distribution has no evident dependence on thermal treatment. The observed variations are probably caused by the heterogeneous foams' macrostructure. On the other hand, it appears that the mechanical properties of Ti-Nb-Zr foams are significantly sensitive to thermal treatment promoting $\beta \leftrightarrow \alpha''$ stress-induced martensitic transformation.

Acknowledgements

This work was supported by the Ministry of Economic Development of Quebec, the National Science and Engineering Research Council of Canada and the Ministry of Education and Science of the Russian Federation.

References

[1] Y.L. Hao, S.J. Li, S.Y Sun, C.Y. Zheng, Q.M. Hu, R. Yang, Super-elastic titanium alloy with unstable plastic deformation, Appl. Phys. Lett., 87(9) (2005) 091906-091908.

[2] S.J. Li, T.C. Cui, Y.L. Hao, R. Yang, Fatigue properties of a metastable β-type titanium alloy with reversible phase transformation, Acta Biomater., 4 (2008) 305-317.

[3] A.K. Mishra, J.A. Davidson, P. Kovacs, R.A. Poggie, Ti–13Nb–13Zr: a new low modulus, high strength, corrosion resistant near-beta alloy for orthopaedic implants, in: ed. by D. Eylon, R. Boyer, D. Koss, Beta Titanium in the 1990's, Warrendale: The Minerals, Metals &Materials Society, 1993, 61-72.

[4] M. Niinomi, Fatigue performance and cyto-toxicity of low rigidity titanium alloy, Ti–29Nb–13Ta–4.6Zr, Biomater., 24 (2003) 2673-2683.

[5] C. Zou, E. Zhang, M. Li, S. Zeng, Preparation, microstructure and mechanical properties of porous titanium sintered by Ti fibres, J. of Mater. Sci.: Mater. in Medicine 19 (2008) 401-405.

[6] A. Schuh, J. Luyten, R. Vidael, W. Ho¨nle, T. Schmickal, Porous titanium implant materials and their potential in orthopedic surgery, Materialwissenschaft und Werkstofftechnik, 38 (12) (2007) 1015-1018.

[7] H. Kim, Y. Ikehara, J. Kim, H. Hosoda, S. Miyazaki, Martensitic transformation, shape memory effect and superelasticity of Ti-Nb binary alloys, Acta Mater. 54(9) (2006) 2419-2429.

[8] S. Miyazaki, H.Y. Kim, H. Hosoda, Development and characterization of Ni-free Ti-base shape memory and superelastic alloys, Mater. Sci. Eng., A. 438-440 (2006) 18-24.

[9] E.W. Collings, Titanium alloys, ed. A.S.f. Metals. 1984.

[10] V. Brailovski, S. Prokoshkin, M. Gauthier, K. Inaekyan, S. Dubinskiy, M. Petrzhik and M. Filonov, Bulk and porous metastable beta Ti-Nb-Zr(Ta) alloys for biomedical applications, Mater. Sci. Eng. C, 31 (2011) 643-657.

[11] V. Brailovski, S. Prokoshkin, K. Inaekyan, S. Dubinskiy, M. Gauthier, Mechanical Properties of Thermomechanically-Processed Metastable Beta Ti-Nb-Zr Alloys for Biomedical Applications Thermec 2011 Proceedings, in press.

[12] S. Prokoshkin, V, Brailovski, K. Inaekyan, A. Korotitskiy, S. Dubinskiy, M. Filonov and M. Petrzhik, A Comparative Study of Structure Formation in Thermomechanically Treated Ti-Ni and Ti-Nb-(Zr, Ta) SMA, Thermec 2011 Proceedings, in press.

[13] United States Patent Number 6,660,224 (US Patent Application Serial Number 09/938,638) filed August 27, 2001, titled "Method of Making Open Cell Material" by inventors Louis-Philippe Lefebvre and Yannig Thomas.

[14] M.F. Ashby, A.G. Evans, .A. Fleck, L.J. Gibson, J.W. Hutchinson and H.N.G. Wadley, Metal Foam: A Design Guide., Butterworth-Heinemann, Boston, 2000.